Manuscript Information

Journal name:	Journal of controlled release : official journal of the Controlled Release Society
NIHMS ID:	NIHMS508830
Manuscript Title:	A Genetically Engineered Thermally Responsive Sustained Release Curcumin Depot to Treat Neuroinflammation
Principal Investigator:	
Submitter:	Author support, Elsevier (ElsevierNIHsupport@elsevier.com)

Manuscript Files

Type	Fig/Table #	Filename	Size	Uploaded
manuscript		COREL_6789.pdf	702435	2013-07-23 06:26:26
supplement	01	mmc1.pdf	1160424	2013-07-23 06:26:28
citation		508830_cit.cit	167	2013-07-23 06:26:26

Title: A Genetically Engineered Thermally Responsive Sustained Release Curcumin Depot to Treat Neuroinflammation

Authors: S. Michael Sinclair, Jayanta Bhattacharyya, Jonathan R. McDaniel, David M. Gooden, Ramesh Gopalaswamy, Ashutosh Chilkoti, Lori A. Setton

PII: S0168-3659(13)00379-9
DOI: http://dx.doi.org/10.1016/j.jconrel.2013.06.032
Reference: COREL/6789

Published in: *Journal of Controlled Release*

Received date: 1 March 2013
Accepted date: 25 June 2013

Cite this article as: Sinclair S M, Bhattacharyya J, McDaniel JR, Gooden DM, Gopalaswamy R, Chilkoti A, Setton LA, A Genetically Engineered Thermally Responsive Sustained Release Curcumin Depot to Treat Neuroinflammation, *Journal of Controlled Release*, http://dx.doi.org/10.1016/j.jconrel.2013.06.032

A Genetically Engineered Thermally Responsive Sustained Release Curcumin Depot to Treat Neuroinflammation

S. Michael Sinclair[1], Jayanta Bhattacharyya[1], Jonathan R. McDaniel[1], David M. Gooden[2], Ramesh Gopalaswamy[2], Ashutosh Chilkoti[1], and Lori A. Setton[1,3]

[1]Department of Biomedical Engineering, Duke University, Durham, NC, USA
[2]Department of Chemistry, Duke University, Durham, NC, USA
[3]Department of Orthopaedic Surgery, Duke University, Durham, NC, USA

AUTHOR EMAIL ADDRESSES

Sinclair – michael.sinclair@duke.edu
Bhattacharyya – jayanta.bhattacharyya@duke.edu
McDaniel – jonathan.mcdaniel@duke.edu
Gooden – david.gooden@duke.edu
Gopalaswamy – ramesh.g@duke.edu
Chilkoti – chilkoti@duke.edu
Setton – setton@duke.edu

AFFILIATION ADDRESSES

Department of Biomedical Engineering
136 Hudson Hall
Box 90281
Durham, NC 27708

Department of Chemistry
Duke University
Box 90354
Durham, NC 27708

Department of Orthopaedic Surgery
DUMC 2887
Durham, NC 27710

RUNNING TITLE

A Thermally Responsive Curcumin Depot for Neuroinflammation

CORRESPONDING AUTHOR

Please send correspondence to Lori A. Setton: 136 Hudson Hall Box 90281, Duke University, Durham, NC 27708 USA. Email: setton@duke.edu Fax: 919-681-8490 Phone: 919-660-5141

ABSTRACT

Radiculopathy, a painful neuroinflammation that can accompany intervertebral disc herniation, is associated with locally increased levels of the pro-inflammatory cytokine tumor necrosis factor alpha (TNFα). Systemic administration of TNF antagonists for radiculopathy in the clinic has shown mixed results, and there is growing interest in the local delivery of anti-inflammatory drugs to treat this pathology as well as similar inflammatory events of peripheral nerve injury. Curcumin, a known antagonist of TNFα in multiple cell types and tissues, was chemically modified and conjugated to a thermally responsive elastin-like polypeptide (ELP) to create an injectable depot for sustained, local delivery of curcumin to treat neuroinflammation. ELPs are biopolymers capable of thermally-triggered in situ depot formation that have been successfully employed as drug carriers and biomaterials in several applications. ELP-curcumin conjugates were shown to display high drug loading, rapidly release curcumin in vitro via degradable carbamate bonds, and retain in vitro bioactivity against TNFα-induced cytotoxicity and monocyte activation with IC_{50} only two-fold higher than curcumin. When injected proximal to the sciatic nerve in mice via intramuscular (i.m.) injection, ELP-curcumin conjugates underwent a thermally triggered soluble-insoluble phase transition, leading to in situ formation of a depot that released curcumin over 4 days post-injection and decreased plasma AUC 7-fold.

KEYWORDS

Curcumin, conjugate, elastin-like polypeptide, sustained release, drug depot, neuroinflammation

1. INTRODUCTION

Intervertebral disc (IVD) herniation, or “ruptured disc,” is a common cause of low back pain that can cause significant back pain, radiating leg pain (a.k.a. sciatica or radiculopathy), neurological impairments, prolonged patient disability, and lost wages [1-3]. Painful symptoms from IVD herniation are believed to result from compression of the nerve root by extruded or prolapsed tissue, an inflammatory response to soluble factors within the IVD, or a combination of these two pathophysiologies [4-7]. At the biological level, radiculopathy and peripheral nerve injury are both characterized by neuroinflammation, immune system activation, and neuronal dysfunction [4, 8, 9]. Following injury, resident macrophages called microglia in the spinal cord and dorsal root ganglion (DRG) are activated and release inflammatory cytokines, chemokines, and neurotransmitters that contribute to pain sensitization [10-12]. These biochemical signals attract peripheral immune cells, which infiltrate the injured nerve site, DRG, or ruptured disc and contribute to chronic inflammation and pain over time [9, 13, 14].

Tumor necrosis factor alpha (TNFα) is a pro-inflammatory cytokine implicated as a key mediator of immune activation and neuroinflammation in radiculopathy and peripheral nerve injury. TNFα is secreted by multiple cell types in response to these injuries, both at the injury site and upstream in the DRG [15, 16], and these responses are, in part, regulated by nuclear factor kappa B (NF-κB) activation [17]. TNFα is expressed at higher levels in degenerated and herniated IVDs [18-23], and application of exogenous TNFα to lumbar DRG in the rat [24, 25], much like animal models of compression-induced nerve root injury, can produce changes in nerve conduction velocity, microglial activation, and inflammatory mediator levels [24, 26].

The central role of TNFα in animal models of neuroinflammation has led to clinical interest in the delivery of TNFα-blocking antibodies and TNFα antagonists to treat IVD herniation-associated pain. However, the high costs and poor clinical results associated with systemic delivery of antibodies or soluble receptors to antagonize TNFα have motivated interest in local drug delivery approaches [27-

30], as well as alternative small-molecule compounds such as minocycline [31], neurotransmitter receptor antagonists [32, 33], and resveratrol [34].

One such compound that has generated significant interest is curcumin, a natural product derived from the rhizome (turmeric) of the herb *Curcuma longa* with known anti-carcinogenic, anti-bacterial, and anti-inflammatory activities [35]. At micromolar concentrations, curcumin suppresses TNF-induced or IL-1-induced activation of NF-κB and downregulates cell adhesion molecules and pro-inflammatory cytokines in multiple cell lines [36-43]. Recently, curcumin has been shown to be a potent modulator of the microglial transcriptome with an ability to alter the activation, migration, and pro-inflammatory phenotype of microglia [44], cells which have been shown to be key initiators of neuroinflammatory pathology in models of radiculopathy and nerve injury [9, 10]. In addition to promoting a neuroprotective phenotype in microglia, curcumin demonstrates neuroprotective activity against IL-1β in rat DRGs at micromolar levels [45] and ameliorates neuropathic pain sensitivities in a mouse model of peripheral nerve injury [46]. Clinically, curcumin suffers from exceptionally low bioavailability due to low solubility and poor absorption into systemic circulation [47]. Many investigators have sought to make curcumin more soluble in aqueous solutions by developing structural derivatives [48-52], or incorporating insoluble curcumin particles into soluble nanoparticles [53]. To prolong systemic circulation of curcumin, investigators have entrapped curcumin in micro- or nano-sized polymeric particles including poly(N-isopropylacrylamide) (poly(NIPAAM)) (i.e. nanocurcumin" [54, 55]), liposomes [56], micellar di-block copolymers [57-59], PLGA microspheres [60, 61], phosphatidylcholine-based phytosomes (Meriva®, Indena S.p.A., Milan, Italy) [62], and self-assembling peptide hydrogels [63]. Curcumin has also been chemically conjugated to drug carriers like poly(ethylene glycol) (PEG) [64], poly(amidoamine) (PAMAM) dendrimers [65], and incorporated into the polymer backbone of a hydrogel system via degradable carbonate bonds [66].

In this study, curcumin was chemically modified to include a degradable carbamate linkage and a reactive primary amine, so that it could be coupled to a thermally responsive drug carrier, an elastin-like polypeptide (ELP), for local, sustained release of bioactive curcumin to treat neuroinflammation. ELPs are thermally responsive biopolymers composed of a Val-Pro-Gly-Xaa-Gly pentapeptide repeat unit that is found to recur in tropoelastin, where Xaa can be any amino acid [67, 68]. ELPs undergo an inverse phase transition at a specified transition temperature (T_t), above which the ELP transitions from a soluble chain to an insoluble, viscous coacervate [69]. The T_t of a given ELP is primarily a function of amino acid composition, solution concentration, and molecular weight, but also depends on the solution pH, ionic strength, polarity of the solvent, and the presence of any fused proteins or conjugated molecules. ELPs have been employed as drug carriers and biomaterials in a variety of applications owing to its facile recombinant synthesis, biocompatibility, biodegradability, and non-immunogenic nature [70, 71]. In prior work, ELPs engineered to form depots at body temperature (T_t < 37 °C) were observed to reside in the perineural space of rats 7 times longer and reduce systemic exposure 14-fold compared to non-depot forming ELP [72]. ELPs have also been useful in forming intratumoral depots for local delivery of radionuclides [73, 74], as well as subcutaneous depots for systemic delivery of glucagon-like peptide-1 for treatment of diabetes [75]. For these reasons, we designed a biodegradable ELP-curcumin conjugate that would rapidly form a depot upon physiological administration and slowly release bioactive curcumin within the perineural space to treat neuroinflammation. This paper reports on the synthesis, physicochemical characterization, in vitro bioactivity, and in vivo pharmacokinetics and clearance rates of the conjugate.

2. MATERIALS AND METHODS

2.1 Materials and Reagents

All reagents were purchased from Sigma Aldrich (St. Louis, MO), unless otherwise noted. 1-Ethyl-3-[3-dimethylaminopropyl]carbodiimide (EDC), sulfo-N-hydroxysulfosuccinimide acetate (sulfo-NHS-acetate), and SnakeSkin® Pleated Dialysis Tubing (MWCO 7000 Da) were purchased from

Pierce Biotechnology (Rockford, IL). Curcumin (95% purity) was purchased from Alfa Aesar (Ward Hill, MA), and fetal bovine serum (FBS) and phosphate-buffered saline (1X PBS) were purchased from Invitrogen (Gibco®, Carlsbad, CA).

2.2 Chemical synthesis of Monofunctional Curcumin Carbamate (MCC)

See supplementary section S.1.

2.3 UV-VIS characterization of curcumin and MCC

The absorbance of curcumin and MCC standards was measured via UV-Vis spectrophotometry from 200 to 800 nm (CARY Bio 300 UV-VIS, Agilent Technologies, Santa Clara, CA). The molar extinction coefficient of MCC at λ_{max} = 416 nm (ε_{416}) was calculated for MCC samples diluted from 100% acetonitrile (CH_3CN) stocks into a cold UV-Vis buffer (50% CH_3CN: 50% DI H_2O, pH = 7.4). ELP was acetylated (AcELP) in a process described below, and AcELP was added to each MCC standard in a fixed molar ratio of 1 mole AcELP to 5 moles MCC to mimic ELP-MCC conjugates, as the presence of proteins such as albumin [76] have been shown to affect curcumin absorbance. Absorbance of MCC with AcELP at 416 nm (OD_{416}) was obtained and plotted against the known concentration of MCC, and ε_{416} was determined from the linear regression of OD_{416} and concentration.

2.4 Conjugate synthesis and purification

Glutamate-rich ELPs with the amino acid sequence MSKGPG[VPGXG]$_{L=60,80,160}$WPC with X = V/I/E [1:3:1] (MW = 26.3, 34.9, and 68.8 kDa), where L is the number of total pentapeptide repeats, were synthesized, expressed, and purified as previously described [77, 78]. Hydrophilic glutamate residues were periodically and precisely placed along the polymer backbone to provide carboxylates convenient for drug attachment; and we hypothesized that unreacted carboxylates remaining after conjugation would compensate for the increase in hydrophobicity following conjugation of curcumin (distribution coefficient at pH = 7.4, log$D_{pH=7.4}$ = 2.9).

2.4.1 Acetylation of ELP terminal amines

To prevent intra- and inter-ELP chain crosslinking, the two terminal amine groups present on purified ELP (the amino terminus and the ε -amine of lysine) were blocked by reacting ELP in 1X PBS (pH = 8.3) at a concentration of 1 mM with sulfo-NHS-acetate (Pierce) dissolved in dimethylformamide (DMF) at a molar ratio of 25 to 1 acetates to amines for 1 h at room temperature. The reaction solution was dialyzed against de-ionized H_2O (DI H_2O, pH = 7.1-7.4) for 48 h with at least 2 buffer changes, and the dialysate was frozen and lyophilized.

Blocking efficiency was confirmed with a 2,4,6-trinitrobenzene sulfonic acid (TNBS) assay [79]. Dry AcELP and unmodified ELP were weighed and dissolved in a known volume of 0.1 M sodium bicarbonate ($NaHCO_3$, pH = 8.3). AcELP was diluted to 50 μM and a standard curve of unmodified ELP ranging from 10-100 μM was prepared. TNBS acid stock was diluted to 0.01% acid in the same buffer and 50 μl was added to 50 μl of sample or standard in a 96-well plate. The plate was incubated at 60 °C (15 min.), allowed to cool at room temperature (5 min.), and absorbance was recorded at 340 nm (background correction at 595 nm) (Enspire Multimode Plate Reader, Perkin Elmer, Waltham, MA). Successful blocking was defined as a reduction in 340 nm absorbance by ≥ 90% of unmodified ELP. This process resulted in a net increase in molecular weight of 43 Da per acetyl group, or 86 Da per ELP.

2.4.2 Conjugate synthesis

ELP-MCC (AcELP$_{L=60,80,160}$) conjugates were synthesized via carbodiimide coupling chemistry and termed MCC60, MCC80, or MCC160. Briefly, dried AcELP, MCC, hydroxybenzotriazole (HOBt), and EDC were individually weighed and dissolved in DMF to insure a ratio of 6 moles MCC for 1 mole AcELP. To the mixture of AcELP and MCC, HOBt and EDC in DMF were added in a 1.5 to 1 molar

ratio to MCC to react carboxylates of AcELP with the amines of MCC. Reaction solutions were rotated at 4 °C in the dark for 18-24 h. Reaction solutions were purified by dialyzing against pre-chilled DI H_2O (pH = 7.1-7.4) for 24 h with 3 buffer changes. The dialyzed conjugate was centrifuged (13.5 kRPM, 10 min., 4 °C) to remove insoluble components, frozen, and lyophilized. Purity was determined by high-pressure liquid chromatography (HPLC), described below.

2.5 Drug-to-carrier ratio characterization

A molar drug:carrier ratio for the ELP-MCC conjugate was determined as described here. A mass of ELP-MCC (m) was dissolved in a known volume of UV-VIS buffer, and absorbance at 416 nm (OD_{416}) and MCC MW were used to obtain the moles of MCC (n_{MCC}) and mass of MCC (m_{MCC}). A value for moles of AcELP in this solution (n_{AcELP}) was determined from the dry weight attributed to AcELP (m-m_{MCC}) and the AcELP MW. The molar drug:carrier ratio was thus reported as n_{MCC}/n_{AcELP}.

2.6 Thermal characterization of conjugates

The thermal transition properties of ELP, AcELP, and ELP-MCC conjugates were measured by monitoring the optical density, or turbidity, of the solution at 650 nm on a thermally controlled UV-Vis spectrophotometer (CARY Bio 300 UV-VIS) as described previously [80]. OD_{650} was selected because curcumin does not absorb light at that wavelength. Samples were diluted in 1X PBS (pH = 7.4) to 25 μM ELP and OD_{650} was monitored from 20 to 80 °C with a temperature ramping rate of 1 °C/min. The transition temperature (T_t) was defined as the point at which the derivative of OD_{650} with respect to temperature was at its maximum value.

The mean particle diameters of ELP-MCC conjugates (25 μM in 1X PBS, pH = 7.4)) were measured using dynamic light scattering (DLS, Zetasizer Nano ZS, Malvern Instruments, Malvern, Worcestershire, UK). Any particle subpopulation representing less than 2% of the total mass was excluded from analysis, and data were reported as the mean particle diameters with standard error representing the calculated polydispersity at each temperature.

2.7 In vitro drug release and quantitation (HPLC)

In vitro drug release and conjugate purity was measured by reverse-phase HPLC (RP-HPLC) (LC10, Shimadzu, Kyoto, Japan) using a Phenomenex Aeris™ WIDEPORE XB-C18 column (4.6 mm X 250 mm) and HPLC mobile phase (50% CH_3CN: 50%DI H_2O: 0.87% acetic acid, CH_3COOH). Samples were injected (100 μl) with a flow rate of 0.6 ml/min and monitored at OD_{420}. Area-under-the-curve (AUC) and percent of total AUC (%AUC) for each peak of the chromatogram were analyzed with Shimadzu EZStart Software.

To quantify the kinetics of MCC release from the ELP-MCC conjugate, samples (MCC80, 50 μM) were diluted in a release buffer (10% (w/v) Tween-80, 0.1% (w/v) N-acetylcysteine (N-Ac), and 0.01% (w/v) butylated hydroxytoluene (BHT) in 1X PBS at pH = 7.4) previously reported to promote stability of curcumin [61]. To this release buffer, 10% FBS was added to test if serum proteins influenced MCC hydrolysis and/or ELP degradation. Conjugates were divided into 50 μl aliquots (25 μM MCC80 or 150 μM MCC) and incubated in the dark at 37 °C. At multiple time points (0, 1, 2, 4, 24, 48, 72, 96 h; n = 4 replicates), one aliquot was removed from heat, cooled on ice to resolubilize ELP (5 min), diluted 1:3 in mobile phase, and stored at -20 °C before analysis. After thawing and before analysis, samples were centrifuged (13.5 kRPM, 10 min, 4 °C) to remove any precipitates.

Aliquots were analyzed via HPLC and converted to concentrations using standard curves for MCC80 and curcumin to determine the curcumin concentration in the supernatant. The resulting concentrations were normalized to the loaded concentration and converted to percent drug released, C, which was plotted as a function of time and fit to a first-order release equation, $C = C_f [1-e^{-t/\tau}]$, to determine the release half-life $t_{1/2} = \ln(2)\tau$. Release data was numerically fit to the above equation (Matlab, function *cftool*) to calculate the fit parameters C_f, the final percent drug released, and $t_{1/2}$.

2.8 In vitro cytoprotection against TNFα

A murine L929 fibrosarcoma (ATCC) cytoprotection assay [81] was used to screen *in vitro* drug bioactivity of curcumin and MCC80 conjugates against TNFα. The assay was performed as previously described [82], with modifications to accommodate the low aqueous solubility of curcumin. Curcumin stocks were prepared in DMSO and MCC80 stocks were prepared in sterile 1X PBS. Cells were pre-incubated with 1 μg/ml of actinomycin D (1 h) after which individual wells were supplemented with 250 pg/ml recombinant human TNFα (rhTNFα) in 2% DMSO (Abcam, positive control), an equivalent media volume with 2% DMSO (negative control), or volumes containing TNFα with MCC80 or curcumin [0.5 to 25 μM].

After 24h incubation, cell numbers were assessed using the ATP-dependent bioluminescent CellTiterGlo® Assay (Promega). A standard curve of luminescence against cell number was obtained using L929 cells (0-50,000 cells/ well) on a plate reader. From luminescence per experimental well, a subtracted cell number per well was determined as the difference between cell number (N) and maximum cell numbers without TNFα or $\Delta N = N - N_{negative}$. A normalized cell fraction, *X*, was calculated for each drug at each dose as $X = \Delta N / \Delta N_{max}$ where ΔN_{max} represents the difference in cell numbers due to TNFα supplementation alone (positive control). *X* was plotted against curcumin or MCC80 concentration and numerically fit to a logistic curve (Matlab, function cftool) to calculate a half-maximal inhibitory concentration (IC_{50}) for curcumin and MCC80, separately,

$$X = \frac{1}{1+\frac{[c]^k}{b}} \quad (1)$$

The Hill slope, k, and b are fit parameters and the IC_{50} (*X* = 0.5) is equal to $b^{(1/k)}$.

2.9 In vitro inhibition of human monocyte NF-kB phosphorylation

Human monocytes (U937, ATCC) were cultured in suspension in U937 culture medium (RPMI-1640 medium with 10% FBS and 100 μg/ml penicillin and streptomycin) and not allowed to grow to confluence prior to cell seeding. Cells were resuspended in U937 assay medium (Hank's Balanced Salt Solution (HBSS, Gibco) with 1% FBS) and 40 μl of cells were seeded in 96-well plates (400,000 cells/well, n=3 replicates). U937 cells then received 20 μl of U937 assay medium with or without curcumin or MCC80 in 2% DMSO at a high (5 μM) or low (0.5 μM) concentration. Cells were pre-incubated for 2 h at 37 °C. At that time, 20 μl of U937 assay medium with or without rhTNFα (final concentration of 50 ng/ml) was added to each well and incubated for 10 min. at 37 °C. Lysis buffer (20 μl, 5X concentrated) was added to each well, plates were agitated for 10 min. at room temperature, cell lysate (30 μl) was transferred to a fresh 96-well white-bottom plate, and the levels of phosphorylated NF-κB p65 were quantified using an AlphaScreen® SureFire HV™ AlphaLISA (Perkin-Elmer).

Data were normalized to the negative control (no TNFα, no drug) and differences in phosphorylated NF-κB p65 across treatment groups were detected using one-way ANOVA with post-hoc Tukey's HSD tests (JMP10, SAS Institute, Cary, NC, USA).

2.10 In vivo pharmacokinetics and drug clearance rates following perineural delivery

All animal studies were conducted following protocols approved by the Duke Institutional Animal Care & Use Committee. Animals were anesthetized with isoflurane, and curcumin or MCC80 (40 μl, 6mM) was delivered by intramuscular (i.m.) injection using a 50 μl Hamilton syringe with a sterile 27-gauge needle into the left thigh, adjacent to the sciatic nerve of female C57BL/6 mice (12-15 weeks, n = 2 or 3 per group, Charles Rivers Laboratories, Durham, NC). Curcumin was suspended in DMSO and MCC80 was suspended in sterile 1X PBS.

For pharmacokinetic studies, animals were serially bled via the maxillary vein to collect 50-100 μl of whole blood over time (0.5 to 96 h). Blood was collected in EDTA-containing BD Vacutainer® microvials (BD, Franklin Lakes, NJ), inverted, immediately centrifuged (4 °C, 3500 RPM, 15 min), and plasma fractions were transferred to 2 mL cryovials (Corning Inc., Corning, NY) and stored at -80 °C. Protocols for the detection and quantitation of curcumin in plasma can be found in section S.2. The concentration of curcumin in plasma was plotted over time for each animal, and the AUC for each animal (nM*h) was calculated using the trapezoid method for only those time points where curcumin levels were above detection limit. To account for plasma autofluorescence that may contribute to total AUC, a corrective factor, AUC_{naive} = LLD*(final timepoint-initial timepoint), was calculated and subtracted from each individual AUC. These corrected AUC values were used to calculate the mean AUC_{Curc} and mean AUC_{MCC80}.

For clearance studies, the injection site was defined to include the sciatic nerve segment at the mid-thigh (~5-10 mm), muscles dorsal and ventral to the nerve segment, and the dorsal skin and subcutaneous layers surrounding the point of needle entry. Animals were sacrificed at 2, 48, and 96 h by exsanguination to collect blood, after which all tissues from the injection site were harvested. To quantify a maximum recoverable percent of injected dose from tissues at time zero (%ID max), two naïve animals were injected (i.m.) with curcumin or MCC80 just after sacrifice and tissues were immediately harvested. Protocols for the detection and quantitation of curcumin from tissue samples can be found in section S.3. Concentrations of curcumin in tissue samples were converted to mass (nmol) using the known volume of tissue buffer added, mass per grams of tissue (nmol/g), and %ID (nmol/nmol*100%) for comparison.

Differences in plasma concentrations, plasma AUC, and drug masses in harvested tissue (nmol) between curcumin, MCC80, and naïve plasma groups were analyzed by one-way ANOVA (JMP10) with post-hoc Tukey's HSD tests.

RESULTS

3.1 Synthesis of MCC

MCC was successfully synthesized by a 3-step reaction shown in Figure 1. Formation of a reactive carbonate intermediate, followed by reaction of the intermediate with N-boc-ethylenediamine, yielded a mono-protected curcumin carbamate. Analysis of the reaction mixture by thin layer chromatography indicated complete consumption of curcumin, and electrospray ionization mass spectrometry (ESIMS) indicated one peak with the expected mass of the mono-protected curcumin carbamate (m/z = 554 ($[M+H]^+$)). This product was deprotected using standard techniques to yield the desired final product, MCC (Figure S1, ESIMS m/z = 455 ($[M+H]^+$)). The structure of MCC was further confirmed with ^{1}H-NMR (Figure S2).

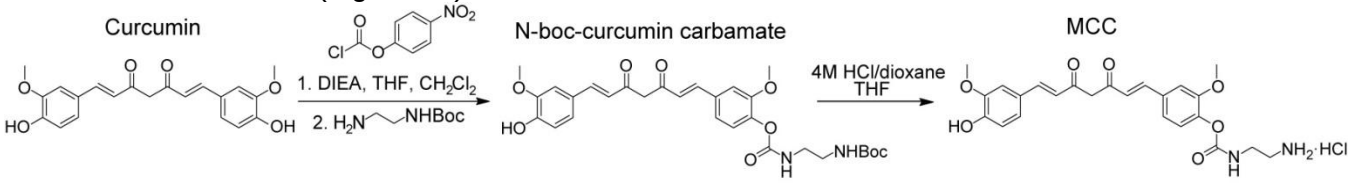

Figure 1. Reaction schematic for the synthesis of MCC from curcumin.

3.2 Absorbance properties of curcumin and MCC

The absorbance spectra of curcumin and MCC in UV-Vis buffer were measured in the presence of AcELP in a molar ratio of 5 to 1 MCC to AcELP (Figure 2). In the presence of AcELP, the wavelength of maximum absorbance, λ_{max}, for curcumin was found to be 425 nm, and λ_{max} for MCC was found to be blue-shifted to 416 nm. At the same concentration, the maximum absorbance of MCC in UV-Vis buffer was 50% lower than for curcumin, indicating the change in structure of MCC hinders its

ability to absorb light. The molar extinction coefficient of MCC at 416 nm, ε_{416}, in the presence of AcELP was calculated to be 31806 $M^{-1}cm^{-1}$.

3.3 Acetylation of ELP N-terminal amines

Glutamate-rich ELPs were reacted with sulfo-NHS-acetate to block the two N-terminal amines present on ELP, which were found to contribute to excessive intra- and inter-chain crosslinking when left unblocked. When sulfo-NHS-acetate was added in large excess (25 moles acetate to 1 mole amine), the reaction resulted in the irreversible addition of an acetyl group (43 Da) to each amine of ELP, which was confirmed for each batch using the TNBS assay.

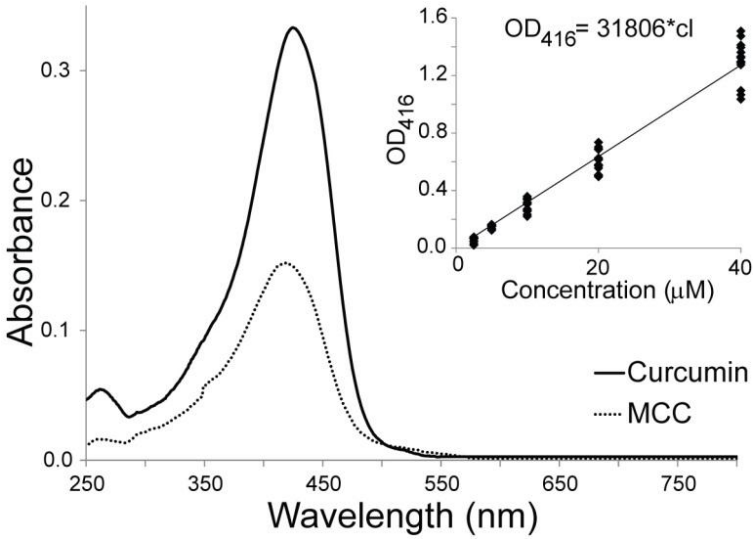

Figure 2. Absorbance spectrum of curcumin and MCC in UV-Vis buffer at the same concentration in the presence of AcELP. (Inset) Linear regression fit of MCC standards to Beers-Lambert law (A = εcl) to calculate ε_{416} for MCC (n = 3 tests, 4 scans per test, $R^2 = 0.9712$).

As the thermal transition temperature (T_t) of ELPs is dependent upon the hydrophobicity of the polymer chain, the addition of small, hydrophilic acetyl groups led to a 2-4 °C increase in the T_t of each AcELP at the concentrations tested (Table 1). Differences in ELP transition kinetics and reversibility were not detected for AcELP compared to unmodified ELP for all sizes.

3.4 Characterization of ELP-MCC conjugates

3.4.1 Drug-to-carrier ratios

The mean drug-to-carrier ratio for MCC60 and MCC80 was 7.2 ± 0.2 and 5.9 ± 0.2, indicating that approximately 5 or 10 glutamates remained unconjugated, respectively (Table 1, mean ± SEM, n=3 batches). Preliminary reactions of MCC with $ELP_{L=160}$ had low yields and ratios below unity, so further studies of MCC160 were not pursued. HPLC was used to verify that there was no more than 5% unreacted MCC or recently released curcumin in each batch for each ELP.

Table 1. Characterization of ELP, AcELP, and ELP-MCC Conjugates

Length, L	MW (kDa)	T_t (ELP) (°C)	Blocking (%)	T_t (AcELP) (°C)	MCC:ELP Ratio	T_t (ELP-MCC) (°C)
60	26.3	>80	72	>80	7.2	54
80	34.8	72	90	76	5.9	40
160	68.7	63	84	65	0.8	39

ELP contain 13, 17, or 33 carboxylic acids, respectively, when including the C-terminus. % blocking for $AcELP_{L=60,160}$ were below 90%, but high and low concentrations of each AcELP were not different from the lowest standard tested. Purity of MCC60 and MCC80 were both ~95%, as measured by HPLC. T_t are reported for 25 μM ELP or AcELP for all cases. Drug-to-carrier ratios for MCC60 and MCC80 represent the mean ratio of n = 3 separate batches.

3.4.2 Thermal transition properties of ELP-MCC conjugates

Curcumin is a highly hydrophobic molecule, and hence was expected to decrease the T_t of ELP-MCC conjugates. ELP-MCC conjugates are thermally responsive, with T_t of 40 °C or 54 °C for MCC80 and MCC60, respectively, at 25 μM. At therapeutically relevant doses (>100 μM ELP), MCC80 conjugates exhibit a T_t ≤ 37°C, which is ideal for *in situ*-gelling therapeutics (Figure 3). The T_t of MCC80 conjugates dropped by 35 °C, or ~6°C/molecule MCC, which is consistent with the reported effects of other hydrophobic molecules, such as doxorubicin, on the T_t of ELP-Dox conjugates [80, 83]. At a concentration of 1 mM, MCC80 conjugate T_t appeared to deviate from the logarithmic dependence of T_t on concentration [84]. The T_t of MCC60 conjugates also dropped significantly, though not enough to be useful for an injectable, local delivery application, even after resuspending at millimolar concentrations. Therefore, MCC60 conjugates were not characterized further or included in pharmacokinetic and clearance studies.

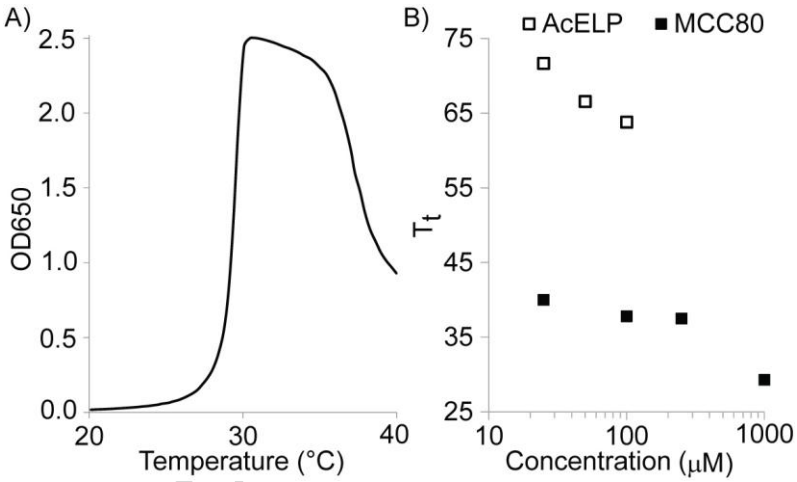

Figure 3. Rapid thermally-triggered phase transition of MCC80 conjugates below physiologic temperatures. A) MCC80 was resuspended at 1 mM conjugate (6 mM MCC) in 1X PBS (pH = 7.4) and heated at a constant rate of 1 °C/min while monitoring the solution turbidity (OD650). B) MCC80 displayed significantly lower T_t than $AcELP_{L=80}$. Concentrations of MCC80 at or above 100 μM exhibited T_t ≤ 37°C.

The mean particle diameters for conjugates were determined by DLS. ELP and AcELP (L=60,80,160) monomers displayed diameters < 20 nm below the T_t and aggregated into submicron-sized particles above the T_t (not shown). Below T_t, MCC80 conjugates were observed as two populations with mean particle diameters of 16.8 nm ± 3.7 nm or 251 nm ± 120 nm, which represented 43% or 57% of the total mass, respectively. Above T_t, the entirety of the sample mass was observed as submicron-sized particles with mean particle diameter of 631 nm ± 50.0 nm (Figure S3).

3.4.3 In vitro release of curcumin from MCC80 conjugates

In vitro release studies of MCC80 conjugates were conducted in a solubilizing release buffer that was modified with 10% FBS, which introduced proteases and esterases likely to impact in vivo release kinetics. MCC80 conjugates released whole-length curcumin with the same elution time and profile as native curcumin using the HPLC methods described here. Curcumin was rapidly released from MCC80 depots in vitro (Figure 4), with 55% of loaded curcumin released after 96 hours at 37°C. The half-life of curcumin release, $t_{1/2}$, from MCC80 depots was calculated to be 7.1 hours.

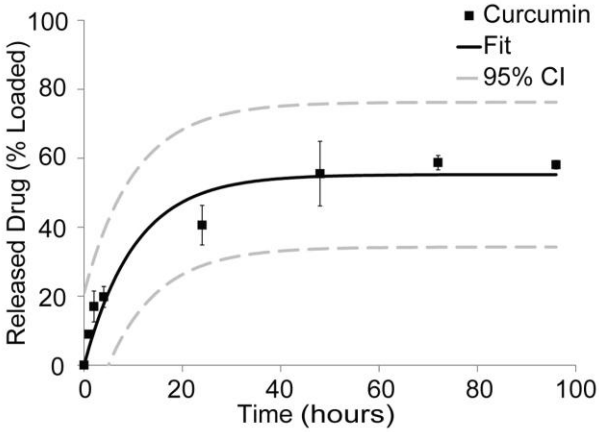

Figure 4. In vitro release of curcumin from MCC80 conjugates in a release buffer with 10% FBS. Numerical fit: R^2 = 0.88; L_{eq} = 55.26 [49.17, 61.35]; $t_{1/2}$ = 7.154 [3.36, 10.9]. Brackets indicate 95% CI.

3.4.4 Dose-dependent cytoprotection of curcumin and conjugates against TNFα

MCC80 conjugates retained bioactivity against TNFα and displayed a dose-dependent ability to protect L929 cells from TNF-induced death (Figure 5). IC_{50} values for curcumin and MCC80 were calculated to be 13.5 μM and 24.1 μM, respectively. The minor decrease in bioactivity of conjugates may be related to the decreased availability of drug trapped in depots or the delayed diffusion of drug to the target cells from depots. It should be noted that no organic solvent (DMSO) was required to solubilize the highest doses of MCC80, which indicated that ELP conjugation results in enhanced curcumin solubility. $ELP_{L=80}$ and $AcELP_{L=80}$ had no effect on L929 cell proliferation over 24 h, but doses of curcumin in DMSO above 30 μM had some cytotoxic effects, owing to the insolubility of the compound at these higher concentrations (not shown).

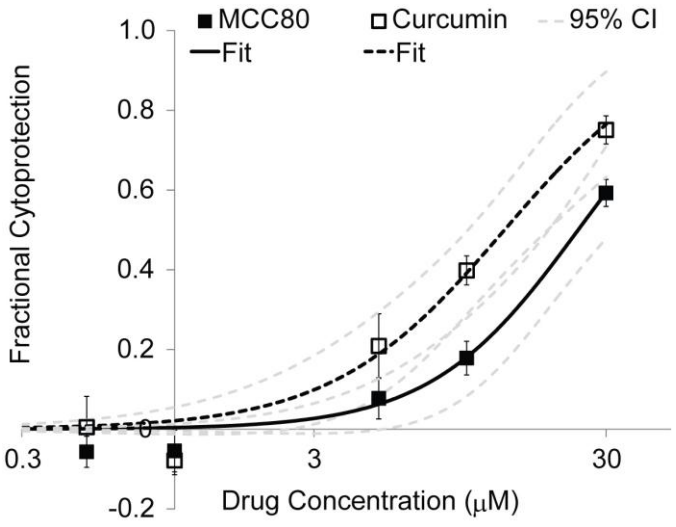

Figure 5. Dose-dependent anti-TNFα bioactivity of MCC80 and curcumin in the L929 cytoprotection assay. Data was fit by nonlinear least-squares regression to Equation 1 to calculate IC_{50} values. The IC_{50} of MCC80 was almost 2-fold higher than curcumin; however, the 95% confidence intervals for each drug overlap substantially. MCC80 numerical fit: b = 237.6; k = 1.72; IC_{50} = 24.1 μM [19.1, 32.0]; R^2 = 0.98. Curcumin numerical fit: b = 45.95; k = 1.472; IC_{50} = 13.5 μM [10.1, 19.0]; R^2 = 0.98. Brackets indicate 95% CI.

3.4.5 Dose-dependent inhibition of monocyte NF-κB phosphorylation

The ability of curcumin and MCC80 to inhibit NF-κB p65 phosphorylation was investigated using an human monocyte cell line (U937) previously used to study the inhibitory effects of curcumin against TNFα [85]. Peak increases in TNF-induced NF-κB phosphorylation was separately observed to occur 10 minutes after exposure to TNFα (not shown). As shown in Figure 6, U937 cells displayed 7.3-fold increases in phosphorylated NF-κB after 10-minute incubation with

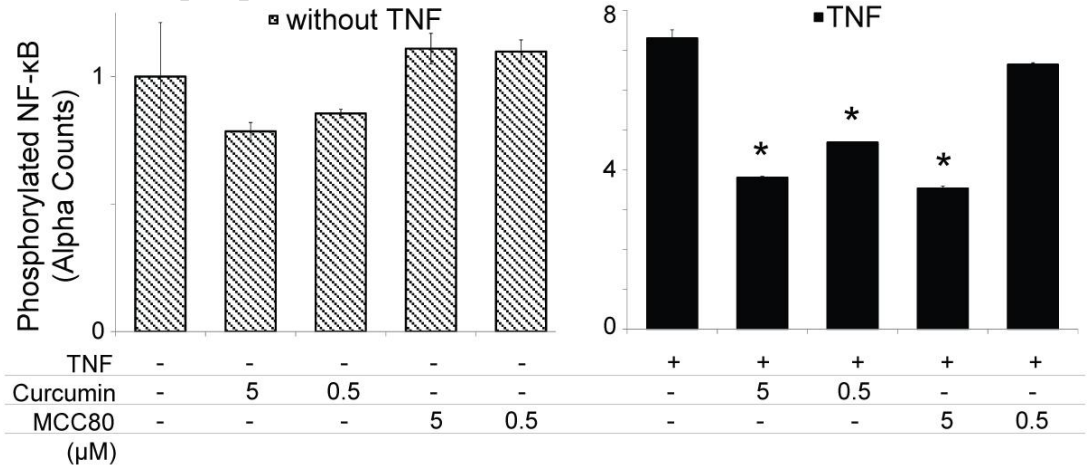

Figure 6. Attenuation of TNF-induced human monocyte NF-κB p65 phosphorylation with curcumin and MCC80. High and low doses of curcumin and MCC80 had no statistically significant effect on basal NF-kB phosphorylation compared to controls, but were able to attenuate TNF-induced increases in NF-kB phosphorylation in a dose-dependent manner (mean ± SEM, n = 3 replicates). * = different from TNF only, one-way ANOVA, $p < 0.0001$.

TNFα (50 ng/ml, n = 3 assays, 1-3 replicates per assay). This TNF-induced activation of monocyte NF-κB was equally attenuated with high micromolar doses of curcumin and MCC80 conjugates (Figure 6).

3.4.6 *In vivo pharmacokinetics and drug clearance rates for MCC80 conjugates*

Curcumin and MCC80 were delivered proximal to the sciatic nerve in mice via i.m. injection and drug levels were tracked in plasma and tissue over time. The lower limit of detection (LLD) for the plasma fluorescence assay was found to be 22 nM for the plate reader assay, which corresponds to a final concentration of 176 nM after accounting for sample dilution. Curcumin was detected in plasma out to 4 h following injection (Figure 7), with maximum plasma levels C_{max} = 590 nM ± 40 nM and 260 nM ± 3.0 nM for free curcumin and MCC80, respectively (n=2 or 3 animals, mean ± SEM). C_{max} levels occurred at a time, t_{max}, of 1-2 h for both curcumin and MCC80, which is similar to oral [86] and subcutaneous delivery [61] of curcumin in mice reported elsewhere. Plasma concentrations for curcumin, MCC80, and naïve plasma for all time-points less than 24 h were statistically different from each other, and AUC_{MCC80} was measured to be 7-fold lower than AUC_{Curc}, indicating that less total curcumin entered the systemic circulation during the first day when it was administered in a depot.

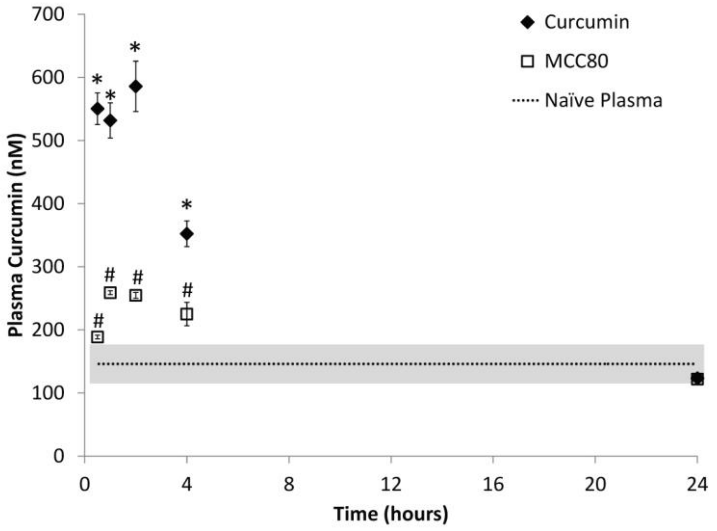

Figure 7. Plasma pharmacokinetics of curcumin following delivery proximal to the sciatic nerve via i.m. injection (n = 2 or 3, mean ± SEM). Naïve plasma mean (146 nM) is plotted ± 2SD [116 nM, 177 nM] in shaded region. Values for curcumin and MCC80 were statistically significant from naïve plasma from 0.5 to 4 h (one-way ANOVA, Jump, $p < 0.0001$). For curcumin: AUC = 870 ± 130 nM*h. For MCC80: AUC = 127 ± 26 nM*h. * = different from naïve plasma and MCC80; # = different from curcumin and naïve plasma.

At 2 h, 48 h, and 96 h, animals were sacrificed to harvest injection site tissue and measure curcumin clearance rates over time. Figure 8 shows the gross appearance of curcumin in DMSO and MCC80 depots proximal to the sciatic nerve 2 h after i.m. injection. Both groups appeared to localize around the sciatic nerve following injection, and MCC80 depots were observed as an orange-yellow gel. Curcumin from MCC80 conjugates cleared from the injection site in a sustained manner. At each time point, MCC80 was detected in depot form by both visual inspection and HPLC analysis of solubilized tissues. Table 2 shows the maximum recoverable mass at time t = 0, as well as the measured masses of curcumin found within tissues at each time point for each group. Based upon the methods reported here, a greater %ID from free curcumin in DMSO delivered by i.m. injection remained at the site of injection at 2 h compared to MCC80, though there was no statistical significance between groups. At this time, free curcumin appeared completely insoluble and in macroscopic particles (Figure 8), indicating that the DMSO vehicle had likely been exchanged for interstitial fluids, rendering curcumin insoluble. This insolubility favored lower initial clearance rates of curcumin compared to MCC80. HPLC analysis of a subset of MCC80 solubilized tissue samples indicated that, for 16 out of 21 samples, >95% of curcumin was still bound to ELP at the time of harvest (not shown). Only samples at 2 h after injection contained a mixed population of free and bound curcumin. At 48 h and 96 h, 5-fold more curcumin was detected for MCC80 compared to free curcumin, and depots of MCC80 were still

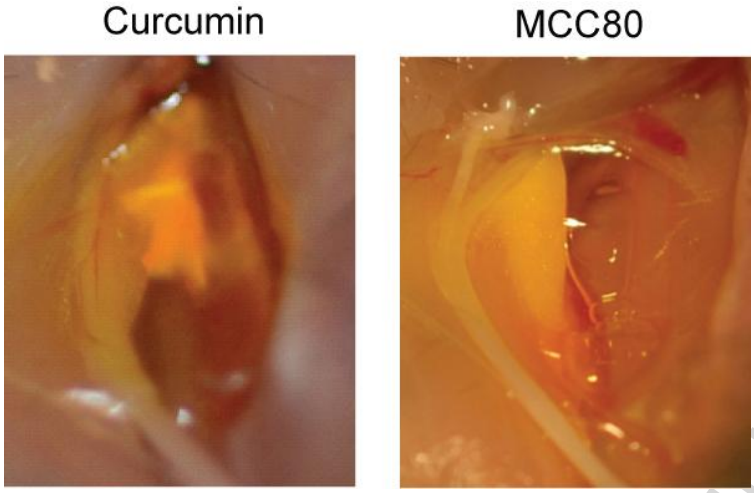

Figure 8. Biopsies of curcumin and MCC80 proximal to sciatic nerve 2 h after i.m. injection. Curcumin in DMSO appears as insoluble aggregates, while MCC80 appears as a soluble gel around the nerve.

visible at 96 h, indicating that conjugation of curcumin to ELP does provide for sustained release of curcumin following local perineural delivery.

3. DISCUSSION

TNFα plays a central role in the local neuroinflammation and pain sensitization associated with radiculopathy and peripheral nerve injury[5, 9], which has led to significant clinical interest in the use of TNF antagonists for treating these conditions [27, 28]. Systemic administration of these drugs has shown minimal efficacy and has motivated efforts to develop local drug delivery strategies that can both increase drug residence time at the site of pain and inflammation and decrease systemic exposure of immunosuppressants [29, 30, 87]. Curcumin is a natural product with an excellent safety profile that has known activity against TNFα via inhibition of NF-κB activation [36]. However, curcumin suffers from low aqueous solubility and bioavailability [47], which has led many investigators to develop drug delivery systems for entrapping or conjugating curcumin to a drug carrier to improve pharmacokinetics and preclinical efficacy [54, 57, 61].

In this study, curcumin was chemically modified and bound to a thermally sensitive ELP biopolymer that experiences a sharp and rapid soluble-to-insoluble phase transition at a temperature below 37 °C [67, 68]. This unique characteristic allows the ELP-curcumin conjugate to be easily handled and injected at room temperature when ELP is fully soluble and then promotes a rapid transition into an immobile viscous coacervate upon warming to physiological temperature. The ELP-curcumin conjugates described here were shown to maintain thermally-triggered depot formation after curcumin conjugation, to readily release curcumin in vitro and in vivo, to retain bioactivity against TNFα, and to contribute to a sustained delivery of curcumin over 4 days following intramuscular injection proximal to the sciatic nerve in mice, while decreasing C_{max} and plasma AUC of curcumin 7-fold. When delivered to less perfused and more isolated compartments, such as the perineural space or epidural

Table 2. Tissue clearance rates for curcumin and MCC80

Group	Time (h)	Mass (nmol)	Mass (nmol/g tissue)	%ID (nmol/nmol)
Curcumin	0*	158	765	59
	2	98 ± 24	531 ± 81	36 ± 8.9
	48[&]	0.67 ± 0.004	7.2 ± 1.3	0.25 ± 0.002
	96	0.39 ± 0.12	2.8 ± 0.95	0.14 ± 0.04
MCC80	0*	90	1080	33
	2	33 ± 8.1	280 ± 73	12 ± 3.0
	48	3.5 ± 1.2	37 ± 10	1.3 ± 0.46
	96	2.2 ± 0.32	15 ± 2.1	0.80 ± 0.12

*=0 h validations were conducted for n=1 animals per group and not included in statistical analyses. All other time points represent n = 3 animals per group (mean ± SEM), except where outliers were removed due to injection error (n = 2[&]). There were no statistical differences between curcumin or MCC80 (one-way ANOVA, p = 0.2).

space, release of curcumin from ELP-curcumin conjugates may be sustained for longer periods and allow for weekly delivery of TNFα antagonists to treat neuroinflammation.

To synthesize ELP-curcumin conjugates, curcumin was first chemically modified to include a reactive primary amine connected by a carbamate linkage, termed monofunctional curcumin carbamate (MCC). With this chemical modification, we generated a more soluble curcumin variant and enabled facile conjugation of curcumin to a variety of carrier compounds with a built-in carbamate bond that is susceptible to hydrolysis and aminolysis [88]. The reported 3-step synthetic schematic employed a carbonate intermediate that can react readily with any primary amine, meaning many modified curcumins could be easily synthesized with distinct carbamate linkers and reactive end-groups. The linker structure of MCC was chosen for its simplicity and as a proof-of-concept of this approach to conjugate design.

The modifications to curcumin reported here had modest effects on the absorbance properties of MCC and somewhat increased the hydrophilicity of curcumin, owing to the hydrophilic carbamate and amine groups. Curcumin has been previously modified by conjugation of single amino acids to form monovalent or divalent curcumin bioconjugates that have increased solubility and anti-microbial or anti-mutagenic bioactivity in vitro [51, 52]. Other investigators have created libraries of curcumin variants by modifying the hydrocarbon backbone and screening these libraries for compounds with increased anti-angiogenic or chemotherapeutic activity [48, 49]. These strategies have proven to be effective methods for increasing curcumin solubility and discovering novel small molecule drugs, and if coupled with sustained drug delivery systems, could prove useful for local delivery applications like neuroinflammation.

We hypothesized that conjugation of curcumin, a very hydrophobic drug, to AcELP would dramatically drop the T_t of AcELP, as was observed for ELP-doxorubicin conjugates [83]. Based upon this hypothesis, highly hydrophilic glutamate-rich ELPs were chosen for this conjugation strategy, which were previously developed for pH-responsive drug delivery applications [78]. The added presence of acetyl groups on ELPs, necessary for MCC conjugation, led to minor increases in T_t, which was expected given the hydrophilicity of acetyl groups. The carboxyl groups of glutamate residues on AcELP were reacted with the primary amines of MCC via carbodiimide chemistry to form ELP-MCC conjugates with a pendant chain structure. As we hypothesized, conjugation of MCC to AcELPs led to an average drop of 6 °C/molecule of MCC. Interestingly, the T_t of MCC80 at 1 mM somewhat deviated from the logarithmic dependence of ELP T_t on concentration previously reported for many ELPs [78, 84]. This observation may be due to the coupling of hydrophobic MCC molecules that likely alter the thermodynamics of ELP aggregation, especially at high concentrations.

In a majority of studies published, micromolar concentrations of curcumin were required to elicit a biological response from a given cell type. Therefore, curcumin must be delivered at high doses in order to be efficacious. The ELP-MCC conjugates reported here were measured to have drug-to-carrier ratios of 6- or 7-to-1 for low- and mid-MW ELP, respectively, and be soluble at millimolar concentrations without the addition of organic solvents. These drug-to-carrier ratios suggest an ability to deliver a releasable form of curcumin at millimolar concentrations directly to the injury site and for sustained periods of time.

The drug-to-carrier ratio of recovered, purified conjugates appears to be limited to these values, however, by the resulting solubility of heavily coupled ELP conjugates. Conjugates formed by reacting at higher MCC-to-ELP ratios were insoluble and could not be purified using the methods described here, which may indicate a substantial drop in T_t or an increased domination of hydrophobic interactions for incremental increases in drug-to-carrier ratio. This limitation could be overcome by redesigning the ELP sequence to make it initially more hydrophilic, or sequestering the reactive carboxyls to one region of the ELP chain (e.g. diblock design). Interestingly, conjugation reactions with large-MW AcELP (L = 160) yielded very low ratios (< 1), which may be related to the lower starting T_t of $AcELP_{L=160}$ compared to the low- and mid-MW AcELPs.

MCC80 conjugates readily released curcumin in vitro when suspended in a stabilizing release buffer. Analysis of release study supernatants with HPLC confirmed that full-length curcumin was released. Given the minor loss of curcumin with each transfer step during the release experiment and HPLC analysis, total curcumin release would never reach 100% of loaded drug using the methods described here. Curcumin released from MCC80 conjugates retained bioactivity against TNFα-induced cytotoxicity in the L929 fibrosarcoma assay and TNFα-induced NF-κB phosphorylation in human U937 monocytes. These results corroborate previous studies of the inhibitory activity of curcumin against TNFα and NF-κB activation in multiple cells types including microglia [44], and suggest that locally delivered curcumin may limit the inflammatory activity of infiltrating macrophages to the site of nerve injury in models of neuroinflammation. In order to test high doses of curcumin, all wells received 2% DMSO, which was shown to not adversely affect cell proliferation. Conjugation of MCC to AcELP increased the solubility of curcumin, such that no DMSO was required for in vitro bioactivity assays or in vivo injections of millimolar concentrations of curcumin. MCC80 conjugates were calculated to have a slightly higher IC_{50} value in the same assay, but the 95% confidence intervals for both drugs overlapped at almost all concentrations. The minor decrease in bioactivity of conjugates may be related to the decreased availability of drug trapped in depots or the delayed diffusion of drug to the target cells from depots.

Other local delivery strategies for curcumin have been developed and studied in vitro, including a curcumin-eluting stent [89], self-assembling peptide hydrogels [63], and incorporation into a hydrogel polymer backbone via degradable carbonate bonds [66]. When curcumin is entrapped rather than conjugated, higher drug loading can be achieved, which may assist with efficacy for applications such as tumor-killing [63]. Incorporation of curcumin into the backbone of PEG-based hydrogels via carbonate bonds led to near zero-order in vitro release kinetics over 80 days, and released curcumin demonstrated cytotoxicity against multiple cancerous cell types [66]. Curcumin could be loaded at high concentrations, while still allowing the hydrogel systems to swell and imbibe water, making these gels a good candidate for local delivery as a soft tissue filler following tumor resection. This study takes these efforts to develop local, sustained drug delivery strategies for curcumin one step further by reporting the in vivo pharmacokinetics and clearance rates of curcumin from a local depot.

The clearance kinetics reported for MCC80 were limited by the method of extraction and detection, as recovery of curcumin and MCC80 at 0 h was only 59% or 33%, respectively. This finding indicates that recovery and quantification of MCC80 in tissues was likely poor for all time points studied, and studies of the clearance rates of MCC80 compared to curcumin require further evaluation. These lower values may reflect, in part, challenges due to extracting curcumin from tissues using solubilization and centrifugation procedures, which were modified from previous pharmacodynamics studies of ELP-doxorubicin [83]. Delivery of ELP-curcumin to a less perfused and more isolated compartment, such as the perineural or epidural space, may facilitate retention of the curcumin in depot form above that which was measured here via i.m. delivery. Furthermore, the extensive previous success of ELP as a drug carrier for subcutaneous, intravenous, intra-tumoral, intra-articular, and perineural delivery are encouraging, and our own visual observations of ELP-curcumin depots at the injection site 4 days after delivery should be emphasized (Figure 8). In the future, the efficacy of local, sustained delivery of ELP-curcumin conjugates to the perineural space in an animal model of neuroinflammation will be investigated.

CONCLUSION

Local delivery strategies for many hydrophobic drugs such as curcumin are becoming more popular to overcome poor bioavailability and achieve a high drug concentration at the site of action, while remaining cost-effective. Likewise, local delivery strategies for treating radiculopathy and peripheral nerve injury are gaining support, given the limitations of systemic administration of TNF inhibitors. We chose curcumin because it possesses a wide range of anti-inflammatory properties relevant to neuroinflammation but has typically limited in vivo efficacy owing to its poor bioavailability

and low solubility. Motivated by these reasons, injectable, thermally-responsive ELP-curcumin conjugates were synthesized and characterized for the purpose of providing local and sustained release of curcumin to treat neuroinflammation pathologies such as IVD herniation-associated radiculopathy or peripheral nerve injury. Upon injection, the physiological temperature triggered the ELP-curcumin conjugate to form depots at the site of administration that displayed a sustained release of bioactive curcumin in vitro and in vivo. ELP-curcumin conjugates retained in vitro bioactivity against TNFα, formed depots in vivo following i.m. injection proximal to the sciatic nerve in mice, and provided sustained, local delivery of curcumin while limiting the systemic exposure of curcumin. However, our strategy to modify and deliver curcumin could be applied to any polyphenol, such as naturally-derived resveratrol, green tea polyphenols, and flavonoids. Furthermore, the MCC linker structure and reactive end-group represent a versatile strategy to couple these drugs to a variety of carriers. In conclusion, ELPs are an excellent drug carrier for such applications, and further studies of in vivo efficacy of ELP-curcumin conjugates in a model of peripheral nerve injury will be investigated.

ACKNOWLEDGEMENTS

This work was funded by the NIH (R01AR047442, P01AR050245, R01AR057410, R01EB000188) and the Duke BME Howard Clark Pre-Doctoral Fellowship.

REFERENCES

[1] W.J. Mixter, J.S. Barr, Rupture of the Intervertebral Disc with Involvement of the Spinal Canal, New England Journal of Medicine, 211 (1934) 210-215.
[2] W.C. Watters Iii, M.J. McGirt, An evidence-based review of the literature on the consequences of conservative versus aggressive discectomy for the treatment of primary disc herniation with radiculopathy, The Spine Journal, 9 (2009) 240-257.
[3] J.N. Weinstein, J.D. Lurie, T.D. Tosteson, A.N.A. Tosteson, E.A. Blood, W.A. Abdu, H. Herkowitz, A. Hilibrand, T. Albert, J. Fischgrund, Surgical Versus Nonoperative Treatment for Lumbar Disc Herniation: Four-Year Results for the Spine Patient Outcomes Research Trial (SPORT), Spine, 33 (2008) 2789-2800 2710.1097/BRS.2780b2013e31818ed31818f31814.
[4] D. Mulleman, S. Mammou, I. Griffoul, H. Watier, P. Goupille, Pathophysiology of disk-related sciatica. I.--Evidence supporting a chemical component, Joint Bone Spine, 73 (2006) 151-158.
[5] K. Olmarker, R.R. Myers, Pathogenesis of sciatic pain: role of herniated nucleus pulposus and deformation of spinal nerve root and dorsal root ganglion, Pain, 78 (1998) 99-105.
[6] M. Kawakami, H. Hashizume, H. Nishi, T. Matsumoto, T. Tamaki, K. Kuribayashi, Comparison of neuropathic pain induced by the application of normal and mechanically compressed nucleus pulposus to lumbar nerve roots in the rat, Journal of Orthopaedic Research, 21 (2003) 535-539.
[7] M. Kawakami, T. Tamaki, J.N. Weinstein, H. Hashizume, H. Nishi, S.T. Meller, Pathomechanism of Pain-Related Behavior Produced by Allografts of Intervertebral Disc in the Rat, Spine, 21 (1996) 2101-2107.
[8] G.A. Loupasis, K. Stamos, P.G. Katonis, G. Sapkas, D.S. Korres, G. Hartofilakidis, Seven- to 20-Year Outcome of Lumbar Discectomy, Spine, 24 (1999) 2313.
[9] J. Scholz, C.J. Woolf, The neuropathic pain triad: neurons, immune cells and glia, Nat Neurosci, 10 (2007) 1361-1368.
[10] H. Hashizume, J.A. DeLeo, R.W. Colburn, J.N. Weinstein, Spinal Glial Activation and Cytokine Expression After Lumbar Root Injury in the Rat, Spine, 25 (2000) 1206-1217.
[11] R.W. Colburn, J.A. DeLeo, A.J. Rickman, M.P. Yeager, P. Kwon, W.F. Hickey, Dissociation of microglial activation and neuropathic pain behaviors following peripheral nerve injury in the rat, Journal of Neuroimmunology, 79 (1997) 163-175.
[12] B.A. Winkelstein, M.D. Rutkowski, S.M. Sweitzer, J.L. Pahl, J.A. DeLeo, Nerve injury proximal or distal to the DRG induces similar spinal glial activation and selective cytokine expression but differential behavioral responses to pharmacologic treatment, The Journal of Comparative Neurology, 439 (2001) 127-139.
[13] M. Doita, T. Kanatani, T. Harada, K. Mizuno, Immunohistologic Study of the Ruptured Intervertebral Disc of the Lumbar Spine, Spine, 21 (1996) 235-241.
[14] Y. Murata, B. Rydevik, K. Takahashi, I. Takahashi, K. Olmarker, Macrophage appearance in the epineurium and endoneurium of dorsal root ganglion exposed to nucleus pulposus, Journal of the Peripheral Nervous System, 9 (2004) 158-164.
[15] M. Schafers, C. Geis, D. Brors, T. Yaksh, C. Sommer, Anterograde transport of tumor necrosis factor-a in the intact and injured rat sciatic nerve, The Journal of Neuroscience, 22 (2002) 536-545.
[16] J. Zhang, Y. De Koninck, Spatial and temporal relationship between monocyte chemoattractant protein-1 expression and spinal glial activation following peripheral nerve injury, Journal of Neurochemistry, 97 (2006) 772-783.

[17] E.S. Fu, Y.P. Zhang, J. Sagen, K.A. Candiotti, P.D. Morton, D.J. Liebl, J.R. Bethea, R. Brambilla, Transgenic inhibition of glial NF-kappa B reduces pain behavior and inflammation after peripheral nerve injury, Pain, 148 (2010) 509-518.
[18] J.D. Kang, H.I. Georgescu, L. McIntyre-Larkin, M. Stefanovic-Racic, W.F. Donaldson Iii, C.H. Evans, Herniated lumbar intervertebral discs spontaneously produce matrix metalloproteinases, nitric oxide, interleukin-6, and prostaglandin E2, Spine, 21 (1996) 271.
[19] C. Le Maitre, J. Hoyland, A. Freemont, Catabolic cytokine expression in degenerate and herniated human intervertebral discs: IL-1 and TNF expression profile, Arthritis Research & Therapy, 9 (2007) R77.
[20] C. Weiler, A.G. Nerlich, B.E. Bachmeier, N. Boos, Expression and distribution of tumor necrosis factor alpha in human lumbar intervertebral discs: a study in surgical specimen and autopsy controls, Spine, 30 (2005) 44.
[21] C.A. Séguin, R.M. Pilliar, P.J. Roughley, R.A. Kandel, Tumor necrosis factor [alpha] modulates matrix production and catabolism in nucleus pulposus tissue, Spine, 30 (2005) 1940.
[22] C.A. Séguin, R.M. Pilliar, J.A. Madri, R.A. Kandel, TNF-[alpha] Induces MMP2 Gelatinase Activity and MT1-MMP Expression in an In Vitro Model of Nucleus Pulposus Tissue Degeneration, Spine, 33 (2008) 356.
[23] C.A. Séguin, M. Bojarski, R.M. Pilliar, P.J. Roughley, R.A. Kandel, Differential regulation of matrix degrading enzymes in a TNF -induced model of nucleus pulposus tissue degeneration, Matrix Biology, 25 (2006) 409-418.
[24] Y. Aoki, B. Rydevik, S. Kikuchi, K. Olmarker, Local Application of Disc-Related Cytokines on Spinal Nerve Roots, Spine, 27 (2002) 1614-1617.
[25] T. Igarashi, S. Kikuchi, V. Shubayev, R.R. Myers, Exogenous tumor necrosis factor-alpha mimics nucleus pulposus-induced neuropathology: molecular, histologic, and behavioral comparisons in rats, Spine, 25 (2000) 2975.
[26] T. Igarashi, S. Kikuchi, V. Shubayev, R.R. Myers, Exogenous Tumor Necrosis Factor-Alpha Mimics Nucleus Pulposus-Induced Neuropathology: Molecular, Histologic, and Behavioral Comparisons in Rats, Spine, 25 (2000) 2975-2980.
[27] S.P. Cohen, N. Bogduk, A. Dragovich, C.C.I. Buckenmaier, S. Griffith, C. Kurihara, J. Raymond, P.J. Richter, N. Williams, T.L. Yaksh, Randomized, Double-blind, Placebo-controlled, Dose-response, and Preclinical Safety Study of Transforaminal Epidural Etanercept for the Treatment of Sciatica, Anesthesiology, 110 (2009) 1116-1126 1110.1097/ALN.1110b1013e3181a1105aa1110.
[28] T. Korhonen, J. Karppinen, L. Paimela, A. Malmivaara, K.-A. Lindgren, C. Bowman, A. Hammond, B. Kirkham, S. Järvinen, J. Niinimäki, N. Veeger, M. Haapea, M. Torkki, O. Tervonen, S. Seitsalo, H. Hurri, The Treatment of Disc Herniation-Induced Sciatica With Infliximab: One-Year Follow-up Results of FIRST II, a Randomized Controlled Trial, Spine, 31 (2006) 2759-2766 2710.1097/2701.brs.0000245873.0000223876.0000245871e.
[29] K.D. Allen, M.F. Shamji, B.A. Mata, M.A. Gabr, P.Y. Hwang, S.M. Sinclair, D.O. Schmitt, W.J. Richardson, L.A. Setton, Kinematic and dynamic gait compensations in a rat model of lumbar radiculopathy and the effects of tumor necrosis factor-alpha antagonism, Arthritis Research & Therapy, [in press] (2011).
[30] J.M. Zanella, E.N. Burright, K. Hildebrand, C. Hobot, M. Cox, L. Christoferson, W.F. McKay, Effect of etanercept, a tumor necrosis factor-alpha inhibitor, on neuropathic pain in the rat chronic constriction injury model, Spine, 33 (2008) 227.
[31] S.M. Rothman, B.B. Guarino, B.A. Winkelstein, Spinal microglial proliferation is evident in a rat model of painful disc herniation both in the presence of behavioral hypersensitivity and following minocycline treatment sufficient to attenuate allodynia, Journal of neuroscience research, 87 (2009) 2709-2717.
[32] X.L. Ding, Y.H. Wang, L.P. Ning, Y. Zhang, H.Y. Ge, H. Jiang, R. Wang, S.W. Yue, Involvement of TRPV4-NO-cGMP-PKG pathways in the development of thermal hyperalgesia following chronic compression of the dorsal root ganglion in rats, Behav Brain Res, 208 (2010) 194-201.
[33] M. Sekiguchi, S. Konno, S. Kikuchi, The effects of a 5-HT2A receptor antagonist on blood flow in lumbar disc herniation: application of nucleus pulposus in a canine model, Eur Spine J, 17 (2008) 307-313.

[34] K. Wuertz, L. Quero, M. Sekiguchi, M. Klawitter, A. Nerlich, S.-I. Konno, S.-I. Kikuchi, N. Boos, The Red Wine Polyphenol Resveratrol Shows Promising Potential for the Treatment of Nucleus Pulposus–Mediated Pain In Vitro and In Vivo, Spine, 36 (2011) E1373-E1384 1310.1097/BRS.1370b1013e318221e318655.
[35] P. Anand, S.G. Thomas, A.B. Kunnumakkara, C. Sundaram, K.B. Harikumar, B. Sung, S.T. Tharakan, K. Misra, I.K. Priyadarsini, K.N. Rajasekharan, Biological activities of curcumin and its analogues (Congeners) made by man and Mother Nature, Biochemical Pharmacology, 76 (2008) 1590-1611.
[36] S. Singh, B.B. Aggarwal, Activation of transcription factor NF-kappaB is suppressed by curcumin (diferuloylmethane), Journal of Biological Chemistry, 270 (1995) 24995.
[37] X. Gao, J. Kuo, H. Jiang, D. Deeb, Y. Liu, G. Divine, R.A. Chapman, S.A. Dulchavsky, S.C. Gautam, Immunomodulatory activity of curcumin: suppression of lymphocyte proliferation, development of cell-mediated cytotoxicity, and cytokine production in vitro, Biochemical Pharmacology, 68 (2004) 51-61.
[38] G.Y. Kim, K.H. Kim, S.H. Lee, M.S. Yoon, H.J. Lee, D.O. Moon, C.M. Lee, S.C. Ahn, Y.C. Park, Y.M. Park, Curcumin Inhibits Immunostimulatory Function of Dendritic Cells: MAPKs and Translocation of NF- B as Potential Targets 1, The Journal of Immunology, 174 (2005) 8116-8124.
[39] C. Jobin, C.A. Bradham, M.P. Russo, B. Juma, A.S. Narula, D.A. Brenner, R.B. Sartor, Curcumin Blocks Cytokine-Mediated NF- B Activation and Proinflammatory Gene Expression by Inhibiting Inhibitory Factor I- B Kinase Activity 1, The Journal of Immunology, 163 (1999) 3474-3483.
[40] A. Kumar, S. Dhawan, N.J. Hardegen, B.B. Aggarwal, Curcumin (diferuloylmethane) inhibition of tumor necrosis factor (TNF)-mediated adhesion of monocytes to endothelial cells by suppression of cell surface expression of adhesion molecules and of nuclear factor- B activation, Biochemical Pharmacology, 55 (1998) 775-783.
[41] S.M. Plummer, K.A. Holloway, M.M. Manson, R.J.L. Munks, A. Kaptein, S. Farrow, L. Howells, Inhibition of cyclo-oxygenase 2 expression in colon cells by the chemopreventive agent curcumin involves inhibition of NF-kB activation via the NIK/IKK signalling complex, Oncogene, 18 (1999) 6013-6020.
[42] M. Shakibaei, G. Schulze-Tanzil, T. John, A. Mobasheri, Curcumin protects human chondrocytes from IL-1 -induced inhibition of collagen type II and 1-integrin expression and activation of caspase-3: An immunomorphological study, Annals of Anatomy, 187 (2005) 487-497.
[43] M. Klawitter, L. Quero, J. Klasen, A. Gloess, B. Klopprogge, O. Hausmann, N. Boos, K. Wuertz, Curcuma DMSO extracts and curcumin exhibit an anti-inflammatory and anti-catabolic effect on human intervertebral disc cells, possibly by influencing TLR2 expression and JNK activity, Journal of Inflammation, 9 (2012) 29.
[44] M. Karlstetter, E. Lippe, Y. Walczak, C. Moehle, A. Aslanidis, M. Mirza, T. Langmann, Curcumin is a potent modulator of microglial gene expression and migration, Journal of Neuroinflammation, 8 (2011) 1-12.
[45] L. Hou, W. Li, X. Wang, Mechanism of interleukin-1 -induced calcitonin gene-related peptide production from dorsal root ganglion neurons of neonatal rats, Journal of neuroscience research, 73 (2003).
[46] X. Zhao, Y. Xu, Q. Zhao, C.-R. Chen, A.-M. Liu, Z.-L. Huang, Curcumin exerts antinociceptive effects in a mouse model of neuropathic pain: Descending monoamine system and opioid receptors are differentially involved, Neuropharmacology, 62 (2012) 843-854.
[47] P. Anand, A.B. Kunnumakkara, R.A. Newman, B.B. Aggarwal, Bioavailability of curcumin: problems and promises, Molecular Pharmaceutics, 4 (2007) 807-818.
[48] B.K. Adams, E.M. Ferstl, M.C. Davis, M. Herold, S. Kurtkaya, R.F. Camalier, M.G. Hollingshead, G. Kaur, E.A. Sausville, F.R. Rickles, Synthesis and biological evaluation of novel curcumin analogs as anti-cancer and anti-angiogenesis agents, Bioorganic & medicinal chemistry, 12 (2004) 3871-3883.
[49] T.P. Robinson, R.B. Hubbard Iv, T.J. Ehlers, J.L. Arbiser, D.J. Goldsmith, J.P. Bowen, Synthesis and biological evaluation of aromatic enones related to curcumin, Bioorganic & medicinal chemistry, 13 (2005) 4007-4013.
[50] S. Mishra, U. Narain, R. Mishra, K. Misra, Design, development and synthesis of mixed bioconjugates of piperic acid-glycine, curcumin-glycine/alanine and curcumin-glycine-piperic acid and their antibacterial and antifungal properties, Bioorganic & medicinal chemistry, 13 (2005) 1477-1486.

[51] S.K. Dubey, A.K. Sharma, U. Narain, K. Misra, U. Pati, Design, synthesis and characterization of some bioactive conjugates of curcumin with glycine, glutamic acid, valine and demethylenated piperic acid and study of their antimicrobial and antiproliferative properties, European Journal of Medicinal Chemistry, 43 (2008) 1837-1846.
[52] K.S. Parvathy, P.S. Negi, P. Srinivas, Curcumin-amino acid conjugates: Synthesis, antioxidant and antimutagenic attributes, Food Chemistry, 120 (2010) 523-530.
[53] Y.M. Lvov, P. Pattekari, X. Zhang, V. Torchilin, Converting poorly soluble materials into stable aqueous nanocolloids, Langmuir: the ACS journal of surfaces and colloids, 27 (2011) 1212.
[54] S. Bisht, G. Feldmann, S. Soni, R. Ravi, C. Karikar, A. Maitra, A. Maitra, Polymeric nanoparticle-encapsulated curcumin ("nanocurcumin"): a novel strategy for human cancer therapy, Journal of Nanobiotechnology, 5 (2007) 3.
[55] B. Ray, S. Bisht, A. Maitra, A. Maitra, D.K. Lahiri, Neuroprotective and neurorescue effects of a novel polymeric nanoparticle formulation of curcumin (NanoCruc) in the neuronal cell culture and animal model: Implications for Alzheimer's Disease, Journal of Alzheimer's disease, 23 (2010) 61.
[56] L. Li, F. Braiteh, R. Kurzrock, Liposome-encapsulated curcumin: in vitro and in vivo effects on proliferation, apoptosis, signaling, and angiogenesis, Cancer, 104 (2005) 1322 - 1331.
[57] Z. Ma, A. Shayeganpour, D.R. Brocks, A. Lavasanifar, J. Samuel, High-performance liquid chromatography analysis of curcumin in rat plasma: application to pharmacokinetics of polymeric micellar formulation of curcumin, Biomedical Chromatography, 21 (2007) 546-552.
[58] M. Gou, K. Men, H. Shi, M. Xiang, J. Zhang, J. Song, J. Long, Y. Wan, F. Luo, X. Zhao, Z. Qian, Curcumin-loaded biodegradable polymeric micelles for colon cancer therapy in vitro and in vivo, Nanoscale, 3 (2011) 1558-1567.
[59] A. Sahu, U. Bora, N. Kasoju, P. Goswami, Synthesis of novel biodegradable and self-assembling methoxy poly(ethylene glycol)-palmitate nanocarrier for curcumin delivery to cancer cells, Acta Biomaterialia, 4 (2008) 1752-1761.
[60] P. Anand, H.B. Nair, B. Sung, A.B. Kunnumakkara, V.R. Yadav, R.R. Tekmal, B.B. Aggarwal, Design of curcumin-loaded PLGA nanoparticles formulation with enhanced cellular uptake, and increased bioactivity in vitro and superior bioavailability in vivo, Biochemical Pharmacology, 79 (2010) 330-338.
[61] K. Shahani, S.K. Swaminathan, D. Freeman, A. Blum, L. Ma, J. Panyam, Injectable sustained release microparticles of curcumin: a new concept for cancer chemoprevention, Cancer Research, 70 (2010) 4443-4452.
[62] G. Belcaro, M.R. Cesarone, M. Dugall, L. Pellegrini, A. Ledda, M.G. Grossi, S. Togni, G. Appendino, Efficacy and safety of Meriva(R), a curcumin-phosphatidylcholine complex, during extended administration in osteoarthritis patients, Alternative Medicine Review, 15 (2010) 337-344.
[63] A. Altunbas, S.J. Lee, S.A. Rajasekaran, J.P. Schneider, D.J. Pochan, Encapsulation of curcumin in self-assembling peptide hydrogels as injectable drug delivery vehicles, Biomaterials, 32 (2011) 5906-5914.
[64] A. Safavy, K.P. Raisch, S. Mantena, L.L. Sanford, S.W. Sham, N.R. Krishna, J.A. Bonner, Design and Development of Water-Soluble Curcumin Conjugates as Potential Anticancer Agentsf, J. Med. Chem, 50 (2007) 6284-6288.
[65] W. Shi, S. Dolai, S. Rizk, A. Hussain, H. Tariq, S. Averick, W. L'Amoreaux, A. El Idrissi, P. Banerjee, K. Raja, Synthesis of Monofunctional Curcumin Derivatives, Clicked Curcumin Dimer, and a PAMAM Dendrimer Curcumin Conjugate for Therapeutic Applications, Organic Letters, 9 (2007) 5461-5464.
[66] N. Shpaisman, L. Sheihet, J. Bushman, J. Winters, J. Kohn, One-Step Synthesis of Biodegradable Curcumin-Derived Hydrogels as Potential Soft Tissue Fillers after Breast Cancer Surgery, Biomacromolecules, 13 (2012) 2279-2286.
[67] D.W. Urry, C.H. Luan, T.M. Parker, D.C. Gowda, K.U. Prasad, M.C. Reid, A. Safavy, Temperature of polypeptide inverse temperature transition depends on mean residue hydrophobicity, Journal of the American Chemical Society, 113 (1991) 4346-4348.

[68] A. Chilkoti, M.R. Dreher, D.E. Meyer, Design of thermally responsive, recombinant polypeptide carriers for targeted drug delivery, Advanced Drug Delivery Reviews, 54 (2002) 1093-1111.
[69] D.W. Urry, The change in Gibbs free energy for hydrophobic association: Derivation and evaluation by means of inverse temperature transitions, Chemical Physics Letters, 399 (2004) 177-183.
[70] J.R. McDaniel, D.J. Callahan, A. Chilkoti, Drug delivery to solid tumors by elastin-like polypeptides, Advanced Drug Delivery Reviews, 62 (2010) 1456-1467.
[71] D.L. Nettles, A. Chilkoti, L.A. Setton, Applications of elastin-like polypeptides in tissue engineering, Advanced Drug Delivery Reviews, 62 (2010) 1479-1485.
[72] M.F. Shamji, L. Whitlatch, A.H. Friedman, W.J. Richardson, A. Chilkoti, L.A. Setton, An injectable and in situ-gelling biopolymer for sustained drug release following perineural administration, Spine, 33 (2008) 748.
[73] W. Liu, J.A. MacKay, M.R. Dreher, M. Chen, J.R. McDaniel, A.J. Simnick, D.J. Callahan, M.R. Zalutsky, A. Chilkoti, Injectable intratumoral depot of thermally responsive polypeptide–radionuclide conjugates delays tumor progression in a mouse model, Journal of Controlled Release, 144 (2010) 2-9.
[74] W. Liu, J. McDaniel, X. Li, D. Asai, F.G. Quiroz, J. Schaal, J.S. Park, M. Zalutsky, A. Chilkoti, Brachytherapy Using Injectable Seeds That Are Self-Assembled from Genetically Encoded Polypeptides In Situ, Cancer Research, 72 (2012) 5956-5965.
[75] M. Amiram, K.M. Luginbuhl, X. Li, M.N. Feinglos, A. Chilkoti, Injectable protease-operated depots of glucagon-like peptide-1 provide extended and tunable glucose control, Proceedings of the National Academy of Sciences, 110 (2013) 2792-2797.
[76] A. Barik, K. Priyadarsini, H. Mohan, Photophysical Studies on Binding of Curcumin to Bovine Serum Albumin, Photochemistry and photobiology, 77 (2003) 597-603.
[77] D.T. McPherson, C. Morrow, D.S. Minehan, J. Wu, E. Hunter, D.W. Urry, Production and Purification of a Recombinant Elastomeric Polypeptide, G-(VPGVG)19-VPGV, from Escherichia coli, Biotechnology Progress, 8 (1992) 347-352.
[78] J.A. MacKay, D.J. Callahan, K.N. FitzGerald, A. Chilkoti, Quantitative Model of the Phase Behavior of Recombinant pH-Responsive Elastin-Like Polypeptides, Biomacromolecules, 11 (2010) 2873-2879.
[79] A.F.S.A. Habeeb, M.Z. Atassi, Enzymic and immunochemical properties of lysozyme. Evaluation of several amino group reversible blocking reagents, Biochemistry, 9 (1970) 4939-4944.
[80] D.Y. Furgeson, M.R. Dreher, A. Chilkoti, Structural optimization of a "smart" doxorubicin-polypeptide conjugate for thermally targeted delivery to solid tumors, Journal of Controlled Release, 110 (2006) 362-369.
[81] K.C. P. Tomkins, D. Webber, G. Bowen, The L929 cell bioassay for murine tumour necrosis factor is not influenced by other murine cytokines, J. Immunol. Methods, 151 (1992) 313-315.
[82] M.F. Shamji, J. Chen, A.H. Friedman, W.J. Richardson, A. Chilkoti, L.A. Setton, Synthesis and characterization of a thermally-responsive tumor necrosis factor antagonist, Journal of Controlled Release, 129 (2008) 179-186.
[83] J. Andrew MacKay, M. Chen, J.R. McDaniel, W. Liu, A.J. Simnick, A. Chilkoti, Self-assembling chimeric polypeptide-doxorubicin conjugate nanoparticles that abolish tumours after a single injection, Nat Mater, 8 (2009) 993-999.
[84] D.E. Meyer, A. Chilkoti, Quantification of the effects of chain length and concentration on the thermal behavior of elastin-like polypeptides, Biomacromolecules, 5 (2004) 846-851.
[85] S. Aggarwal, H. Ichikawa, Y. Takada, S.K. Sandur, S. Shishodia, B.B. Aggarwal, Curcumin (diferuloylmethane) down-regulates expression of cell proliferation and antiapoptotic and metastatic gene products through suppression of IκBα kinase and Akt activation, Molecular pharmacology, 69 (2006) 195-206.
[86] M.H. Pan, T.M. Huang, J.K. Lin, Biotransformation of curcumin through reduction and glucuronidation in mice, Drug metabolism and disposition, 27 (1999) 486-494.
[87] M.F. Shamji, L. Jing, J. Chen, P. Hwang, O. Ghodsizadeh, A.H. Friedman, W.J. Richardson, L.A. Setton, Treatment of neuroinflammation by soluble tumor necrosis factor receptor Type II fused to a thermally responsive carrier, Journal of neurosurgery. Spine, 9 (2008) 221-228.

[88] W.S. Saari, J.E. Schwering, P.A. Lyle, S.J. Smith, E.L. Engelhardt, Cyclization-activated prodrugs. Basic carbamates of 4-hydroxyanisole, Journal of Medicinal Chemistry, 33 (1990) 97-101.
[89] C.J. Pan, J.J. Tang, Y.J. Weng, J. Wang, N. Huang, Preparation, characterization and anticoagulation of curcumin-eluting controlled biodegradable coating stents, Journal of Controlled Release, 116 (2006) 42-49.

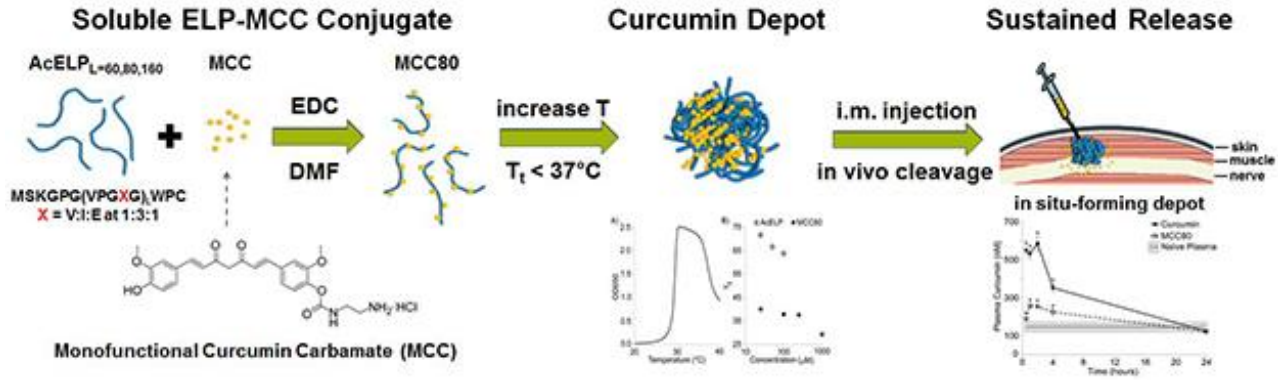

Graphical abstract

The NIHMS has received the file 'mmc1.pdf' as supplementary data. The file will not appear in this PDF Receipt, but it will be linked to the web version of your manuscript.